Asian Journal of Applied Science and Technology (AJAST)
Volume 7, Issue 1, Pages 69-79, January-March 2023

On the Modulation of Biocompatibility of Hydrogels with Collagen and Guar Gum by Adding Molybdenum/ aminoacid-based Metal-organic Frameworks

Martín Caldera-Villalobos[1], Juan C. Martín-Coronado[2], Jesús A. Claudio-Rizo[1*], Denis A. Cabrera-Munguía[1], María I. León-Campos[1], Juan J. Mendoza-Villafaña[1], Lucía F. Cano-Salazar[1] & Tirso E. Flores-Guía[1]

*[1]Facultad de Ciencias Químicas, Universidad Autónoma de Coahuila, Ing. J. Cárdenas Valdez S/N, República, 25280 Saltillo, Coahuila, México. [2]Universidad Autónoma de Aguascalientes, Centro de Ciencias Básicas, Av. Universidad #940, C.P. 20131, Aguascalientes, México. Corresponding Author (Jesús A. Claudio-Rizo) - Email: jclaudio@uadec.edu.mx**

DOI: https://doi.org/10.38177/ajast.2023.7107

Article Received: 19 January 2023 *Article Accepted: 27 February 2023* *Article Published: 14 March 2023*

ABSTRACT

In this work, we report the synthesis of molybdenum metal-organic frameworks (Mo-MOFs) using 1,3,5-benzenetricarboxylic acid and the amino acids L-phenylalanine, L- tryptophan, and L-histidine as ligands. They were incorporated in hydrogel matrixes comprised of collagen and guar gum to obtain composite hydrogels. The effect of chemical structure of Mo-MOFs on the structure, physicochemical properties and in vitro biocompatibility of hydrogels was studied. These biomaterials showed a super absorbent performance (higher than 2000 ± 169%) and a high degree of reticulation (higher than 75 ± 6%). The microstructure of the composites showed a granular morphology with some porosity. These composites were degraded entirely by hydrolysis at pH 5 and pH 7 at room temperature in time lapses shorter than 15 days. Also, they were biocompatible with porcine dermis fibroblasts not showing cytotoxic effects up to 48 h of incubation allowing its proliferation, and it was observed that the MOF containing L-tryptophan improved notably the biocompatibility of the collagen/guar gum matrix. Finally, the matrixes were tested as vehicles for cell encapsulation and release. The slow-release rates show that fibroblasts tend to remain inside the hydrogel matrixes. Thus, these materials are more suitable for cell scaffolds and tissue engineering applications such as wound healing dressings.

Keywords: MOFs; Biomaterials; Biopolymers; Wound healings; Wound dressings; Biotechnology.

1. Introduction

Currently, research using various trace elements such as boron, manganese, vanadium, cobalt, or molybdenum is opening promising avenues in healing therapeutics. For example, the effectiveness of boric acid to improve the performance of wound dressings has been documented by several researchers whose incorporated this compound in fibroin/gelatin films [1], polyurethane sponges [2], and polyamide mats [3].

It was suggested that boric acid could promote the wound healing by a mechanism associated with the increased expression of the transformant growth factor beta (TGF-β) and the deposition of type I collagen [4]. Vanadium-based materials have proved to be effective antibacterials against antibiotic-resistant bacteria [5]. Manganese-doped zeolitic imidazolate framework 8 (ZIF-8) showed enzymatic activity due to the co-existence of Mn^{2}+/Mn^{4+} ions regulating the inflammation in the wound healing process [6].

Moreover, manganese combined with silicon in manganese-doped calcium silicate promotes migration and proliferation of vascular endothelial cells and angiogenesis [7]. Also, a positive effect on the wound healing process has been reported for materials containing cobalt [8-10], and recently some researchers have proved the advantages of molybdenum-based biomaterials.

Molybdenum is the only second transition series metal recognized as essential for living organisms. This element is not abundant in the earth's crust. However, it is present in practically all forms of life, and is of great importance in metabolic processes. Molybdenum is found in around a dozen enzyme systems and is involved in redox processes involving oxygen transfer and nitrogen fixation. Some of the enzyme systems that contain molybdenum are

nitrogenase, aldehyde oxidase, nitrate reductase, sulfite oxidase, xanthine oxidase, and formate dehydrogenase. Molybdenum is found in very low concentrations in almost all body fluids and tissues. It is considered an ultra-micro trace element, since in a 70 kg adult human there are around 0.005 g of this element. Regarding its metabolism, molybdenum is absorbed in the form of MoO_4^{2-} anions relatively quickly and efficiently. Molybdenum in biological systems can vary its oxidation state from Mo (III) to Mo (VI) and can be found with coordination numbers 4 and 6, generating tetrahedral and octahedral structures with oxygen and water molecules, respectively. Further, Mo-OH bonds have also been observed to form and break with relative ease, due to its high chemical lability associated with the electronegativity difference between molybdenum and oxygen [11].

Recently, molybdenum-based materials have been studied as biomaterials potentially applicable for tissue engineering and biomedical applications. For example, a MoO_3-collagen scaffold was found to play an important role in all major events of wound healing such as adhesion, migration, proliferation, and angiogenesis. An in-vivo healing assay proved that the healing rate of animals treated with the MoO_3-collagen scaffold was comparatively faster [12]. In other work, it was demonstrated the immunomodulatory role of a Mo-containing material in dynamic signaling cascade of wound healing, enabling long-term stable macrophage modulation and leading to enhanced regeneration of multiple periodontal tissues in canines [13]. Also, molybdenum metal-organic frameworks (MOFs) synthesized from terephthalic acid and bis(2-hydroxyethyl) terephthalate ligands proved to be biocompatible promoting the proliferation of porcine skin fibroblasts, being potentially applicable for tissue engineering and wound healing [14].

The utility of collagen-based hydrogels as biomaterials capable to accelerate the wound healing process is well known. Also, it was reported that the semi-interpenetration of collagen-polyurethane hydrogels with polysaccharides enhances the biocompatibility and the physicochemical properties of these materials [15]. In a previous work, we studied the effect of the concentration of guar gum (GG) on the biocompatibility of semi-interpenetrating polymer networks (semi-IPNs) based on collagen-GG founding that as the concentration of GG increases the biocompatibility of the resulting hydrogels for porcine fibroblasts increases [16]. Further, we reported that the incorporation of the Zn(Atz)(Py) MOF in the collagen/guar gum hydrogel matrix improves the cell viability of fibroblasts as well as the antibacterial capacity [17]. This work aimed to study the effect of adding molybdenum-based MOFs (Mo-MOFs) (modifying the chemical structure of the amino acid such as phenylalanine, tryptophan, and histidine) on the in vitro biocompatibility of collagen-guar semi-IPN hydrogel, performing in vitro assays to evaluate their potential for wound healing applications.

2. Experimental

2.1. Chemicals

Ammonium heptamolybdate ($((NH_4)_6Mo_7O_{24}\bullet 4H_2O$), 1,3,5-benzenetricarboxylic acid (BTC), L-histidine (His), L-trypthopan (Trp), L-phenylalanine (Phe), guar gum (extracted from Cyamopsis tetragonoloba, M_w = 220 kDa), and 3-(4,5-Dimethyl-2-thiazolyl)-2,5-diphenyl-2*H*-tetrazolium bromide (MTT) were purchased from Sigma-Aldrich Co., and they were used as received. Calcein acetoxymethyl ester (calcein-AM) was purchased from ThermoFischer Scientific. Collagen form porcine dermis was extracted by enzymatic hydrolysis with pepsin as

reported elsewhere (M_n α_1 = 220 kDa, α_2= 110 kDa) [18]. A polyurethane crosslinker was prepared from 1,6-hexamethylene diisocyanate and glycerol ethoxylate as reported elsewhere [19].

2.2. Synthesis of Mo-MOFS

Mo-MOFs were synthesized by the hydrothermal method. For this, 1 mmol of ammonium heptamolybdate, 1 mmol of BTC, and 1 mmol of the suitable amino acid (Trp, Phe, or His) were mixed with magnetic stirring at room temperature. Then, the mixture was transferred to a Teflon-lined autoclave, and the reaction was carried out at 120°C for 72 h. The colorless precipitate obtained from the reaction was filtered, rinsed with water, and dried at 60°C. The obtained MOFs were labeled as Mo(Trp), Mo(Phe), or Mo(His) based on the amino acid used as ligand.

2.3. Preparation of Composite Hydrogels

Previously, a collagen solution (6 mg mL^{-1}) containing 1% wt. of MOF with respect to collagen, and guar gum solution (0.5 % wt.) were prepared. Composite hydrogels were prepared by mixing 1 mL of collagen solution and 15 µL of polyurethane in a culture plate (used as a mold). After that, 120 µL of guar gum solution was added, and after mixing the pH was adjusted to 7 by adding 300 µL of phosphate buffered saline (PBS-10X). The reticulation reaction was carried out by heating at 37°C for 4 h to obtain the hydrogels, which were labeled as ColGG-Mo(Phe), ColGG-Mo(Trp), or ColGG-Mo(His) depending on the MOF used. For the comparison of results, a hydrogel formulation without MOF was prepared (ColGG).

2.4. Characterization

FTIR spectra were recorded using a Perkin-Elmer Frontier spectrophotometer equipped with a total attenuated reflectance accessory (ATR) with a spectral resolution of 4 cm^{-1}. Scanning electron microscopy was performed with a TOPCON SM-510 microscope operated at 10 kV. UV-Vis absorption measurements were performed with a ThermoScientific MultiSkan Sky spectrophotometer. Fluorescence microscopy observations were performed using a VELAB VE146YT microscope using a blue LASER as excitation source (λ = 441 nm).

For the determination of the swelling capacity, the mass of freshly prepared hydrogels was registered. Then, samples were dried at room temperature until obtain a constant mass, measurements were performed in triplicate. The swelling degree was calculated using Equation 1:

$$Swelling\ degree\ (\%) = \frac{m_0 - m_i}{m_i} * 100 \qquad (1)$$

Where m_0 is the initial mass of hydrogels and m_i is the mass of the dried hydrogel, respectively.

The reticulation of semi-IPN hydrogels was analyzed reacting the polymeric matrixes with ninhydrin for 30 min at 90 °C. The absorbance of the liquid phase obtained after completing the reaction was measured by spectrophotometry at 567 nm (samples were prepared in triplicate). Results were compared with unreticulated collagen, and the crosslinking degree was calculated with Equation 2:

$$Crosslinking\ degree\ (\%) = \left(1 - \frac{A_{sample}}{A_{collagen}}\right) * 100 \qquad (2)$$

Where A_{sample} and $A_{collagen}$ are the absorbances of solutions obtained after ninhydrin reacted with hydrogels or unreticulated collagen, respectively.

2.5. Evaluation of the in vitro biocompatibility

The effect of the chemical structure of Mo-MOFs on the metabolic activity of porcine dermis fibroblasts growing in contact with hydrogels was evaluated by the MTT assay. For this, 150 µL of cell suspension (30 000 cells/mL) were seeded over hydrogels in polystyrene culture plates and incubated for 24 and 48 h at 37°C (samples were prepared in triplicate). PBS-1X was used as the positive control. At the evaluation time (24 or 48 h), 15 µL of 3-(4,5-dimetilthiazol-2-yl)-2,5-diphenyltetrazolium) solution (1% wt. in sterilized PBS-1X) was added and incubated for 2 h more. After that, 1 mL of propan-2-ol was added to dissolve the resulting blue formazan crystals. Aliquots of 200 µL were taken from the liquid medium and the absorbance was measured at 560 nm. Cell viability was calculated using Equation 3:

$$Cell\ viability\ (\%) = \frac{A_{sample}}{A_{control}} * 100 \qquad (3)$$

Where A_{sample} and $A_{control}$ represent the absorbances for each sample or formulation and PBS-1X, respectively. Values less than 60% cell viability are considered cytotoxic.

The effect of the composition of Mo-MOFs on the proliferation of fibroblasts was studied by fluorescence microscopy. For this, 1 mL of fibroblasts culture (30 000 cells/mL) was mixed with 1 mL of leaches extracted from semi-IPN hydrogels and incubated at 37°C for 48 h. After incubation, cells were stained with calcein-AM, following the instructions provided by the supplier, PBS-1X was used as the control. Stained cells were transferred to a slide and were inspected with a fluorescence microscope.

2.6. Encapsulation and Release of Porcine fibroblasts

For the encapsulation of porcine dermis fibroblasts, hydrogels were prepared as described previously, but 200 µL of cell culture (30 000 cells/mL) was added to each hydrogel before carrying out the gelation. Then, hydrogels were placed in PBS-1X as releasing medium (10 mL per hydrogel), and then they were incubated at 37°C without stirring. Aliquots of the releasing medium were taken at different time intervals and the absorbance was measured at 558 nm. The experiment was realized in triplicate.

3. Results and Discussions

3.1. Analysis of the Chemical Structure

The chemical structure of Mo-MOFs was analyzed by FTIR spectroscopy, and the acquired spectra are shown in Figure 1. They show some typical bands related to the BTC ligand due to the νC=O, νC-O, and aromatic νC-H vibrations in 1700, 1232, and 3027 cm^{-1}, respectively. The absorption bands in 900 and 734 cm^{-1} were attributed to the Mo=O and Mo-O-Mo vibrations due to the molybdate cluster [20], which are evidence of the incorporation of molybdenum in the MOFs. In the region of 4000-3200 cm^{-1}, it was observed a weakening of the absorption bands due to νO-H and νN-H vibrations, which suggests that carboxylic acid and amino groups are involved in the coordination of the amino acid and BTC ligands with molybdenum. Only a well-defined band was observed in 3458 cm^{-1} in the spectrum of Mo(Trp) due to the νN-H stretching vibration from the indole moiety of Trp, which due to its low basicity is not involved in the coordination with molybdenum as occurring with the imidazole ring of His.

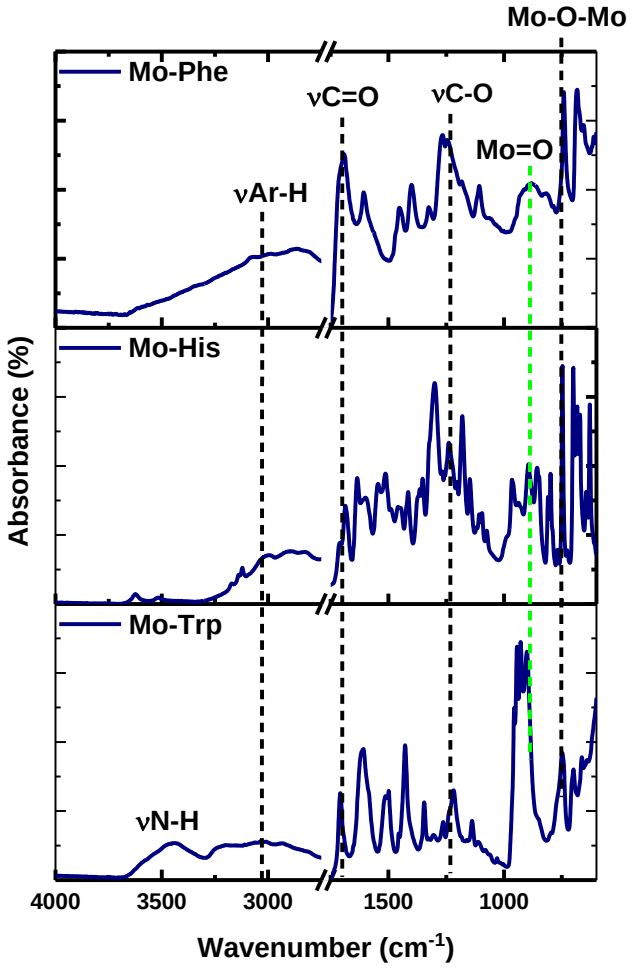

Figure 1. FTIR Spectra of Mo-MOFS

3.2. Swelling and Reticulation Behavior of Composite hydrogels

The effect of molybdenum-based MOFs on the swelling capacity of semi-IPN hydrogels is shown in Figure 2a. The ColGG matrix has a water-absorption capacity of 2651 ± 125% showing a superabsorbent behavior. The addition of Mo(Phe) or Mo(Trp) increases the swelling capacity of the ColGG hydrogel up to 3663 ± 150% for both materials. These results were unexpected due to the hydrophobic character of Phe and Trp conferred by the phenyl and indolyl moieties of each amino acid, respectively. However, hydrophobic repulsion effects allow the matrices to expand for higher absorption of water molecules. Conversely, the composite containing Mo(His) showed lower water-absorption capacity than ColGG although the hydrophilic character of the histidine, indicating that this MOF has better miscibility with the polymeric network, not expanding the chains to improve their swelling.

Figure 2b shows the effect of Mo-MOFs on the reticulation of the ColGG matrix. They increased the reticulation by physicochemical crosslinking involving the formation of covalent bonds and non-covalent interactions such as electrostatic attraction and hydrogen bonding. The covalent reticulation results from the reaction between amino groups occurring in collagen with isocyanate groups occurring in the polyurethane forming urea groups. The physical reticulation involves the electrostatic attraction between negatively charged carboxylate groups occurring in MOFs with positively charged protonated amino groups occurring in collagen (acid-base interaction). Also, the hydrogen bonding between amino, hydroxyl, and carboxylic acid groups contributes to increase the reticulation.

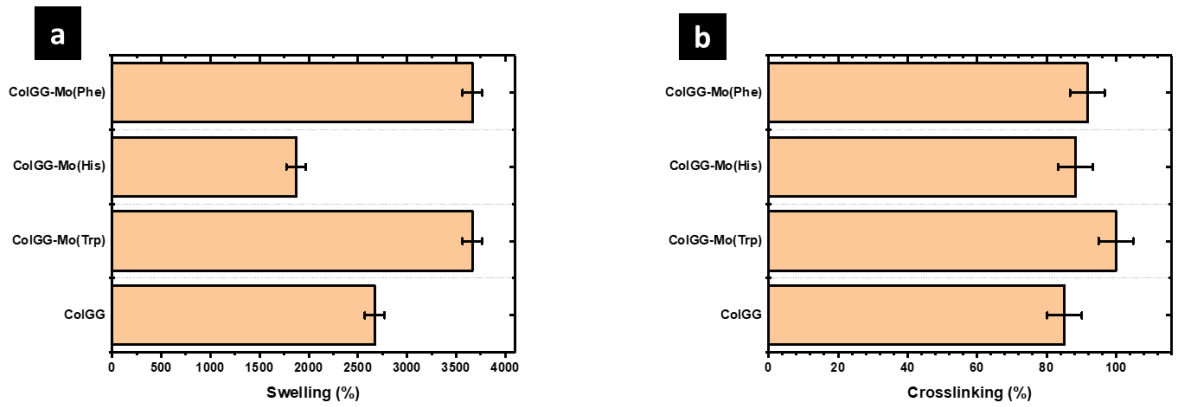

Figure 2. (a) Water-absorption capacity, and (b) Reticulation degree of ColGG-Mo-MOF Composites

3.3. Microstructural Analysis

SEM images reveal the obtaining of porous structures with granular agglomerates resulting from the semi-interpenetration of the collagen-polyurethane matrix with guar gum (Figure 3). This kind of microstructure is highly desirable for biomaterials because matrixes with interconnected porosity have the function as a scaffold where cells adhere and lodge to carry out their vital functions. The chemical structure of the molybdenum-based metal-organic frameworks generates homogeneous surfaces characterized by this porosity. Larger pore size (12 µm) is appreciated for the ColGG-Mo(Trp) composite, which evidences the repulsion of the polymeric chains increasing their water adsorption.

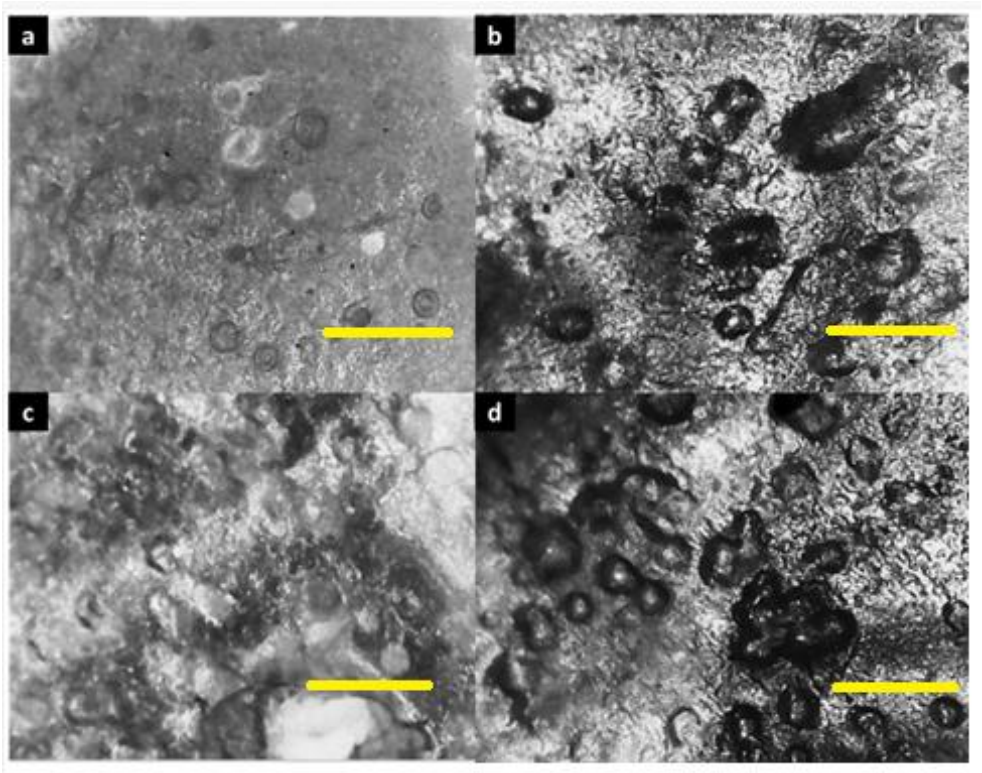

Figure 3. SEM Images Acquired for (a) ColGG, (b) ColGG-Mo(Trp), (c) ColGG-Mo(His), and (d) ColGG-Mo(Phe) - (Scale Bar Equals 10 µm)

3.4. Degradation Behavior

Figure 4 shows the degradation profiles of the composite hydrogels containing Mo-MOFs. At pH 5, it is observed that only Mo(His) is able to retard the degradation process, which occurs mainly by acid hydrolysis of the peptide bond occurring in collagen and urethane groups from collagen. The imidazole ring has a basic character, and it can neutralize the acid medium, retarding the degradation process. After 15 days of contact, a residual mass equivalent to 40% is obtained for ColGG-Mo(His). At pH 7 (PBS-1X), the hydrogels are completely degraded by hydrolysis. The degradation rate decreases in the order ColGG-Mo(Phe) < ColGG-Mo(His) < ColGG-Mo(Trp) < ColGG, showing that Mo(Phe) is the best MOF to retard the degradation of the polymer matrix at this pH. This is associated with the fact that the aromatic ring in phenylalanine is more hydrophilic and acid, which slows down the hydrolysis reactions of this type of biomaterial. The pHs tested in this experiment are typically found in wounds, indicating that the biomaterials show modulation of the rate of degradation. Adapting the rate of degradation as new tissue is formed is important in tissue engineering strategies to avoid the formation of defective tissue.

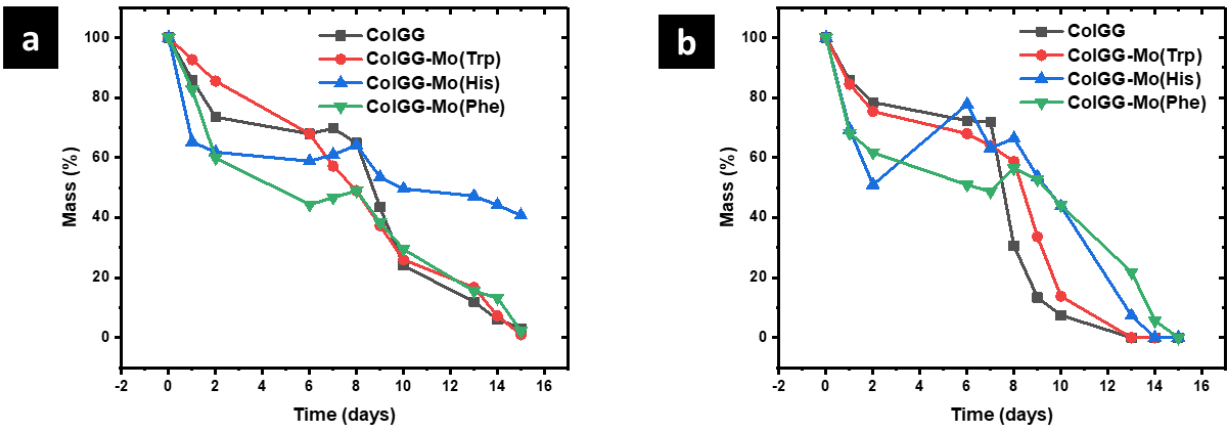

Figure 4. Degradation Profiles for Composite Hydrogels in Hydrolitic Medium: (a) pH = 5 and (b) pH = 7

3.5. Cell Viability and Proliferation

Results obtained from the MTT assay are shown in Figure 5. After 24 h of incubation, the cell viability is higher than 72 ± 5% for all tested materials showing that they have no cytotoxic character for porcine fibroblasts, and thus they are biocompatible. Results show that Mo-MOFs increase to a certain degree the viability of fibroblasts showing that the release of MoO_4^{2-} ions by MOFs stimulates positively the cell metabolism. However, the differences observed between each formulation suggest a differential effect caused by the chemical composition of each MOF associated with the amino acid. In this sense, the best results are obtained with Mo(Trp). Previously, it was reported that Trp has a positive effect at the molecular level on the wound healing process by interacting with the aryl hydrocarbon receptor which is involved in the wound healing process [21]. The topical application of Trp in post-burn wound models showed improved healing represented by smaller wound length, wound area, and increased wound cellularity in a tryptophan-treated group [22]. In other work, it was reported that the Trp administration inhibited the secretion of the tumor necrosis factor alfa (TNF-α) normalizing the inflammatory response of chronically stressed mice. Also, Trp decreases lipid peroxidation and improves myofibroblast differentiation, collagen deposition, re-epithelialization, and wound contraction [23]. In counterpart, reports of

similar activities for Phe and His have been not found. Thus, we can assume that Mo(Trp) is the best MOF for wound healing applications. Considering the antibacterial activity of the imidazole ring, Mo(His) could confer antibacterial properties to the ColGG hydrogel. However, it is necessary to perform the appropriate study to prove this hypothesis.

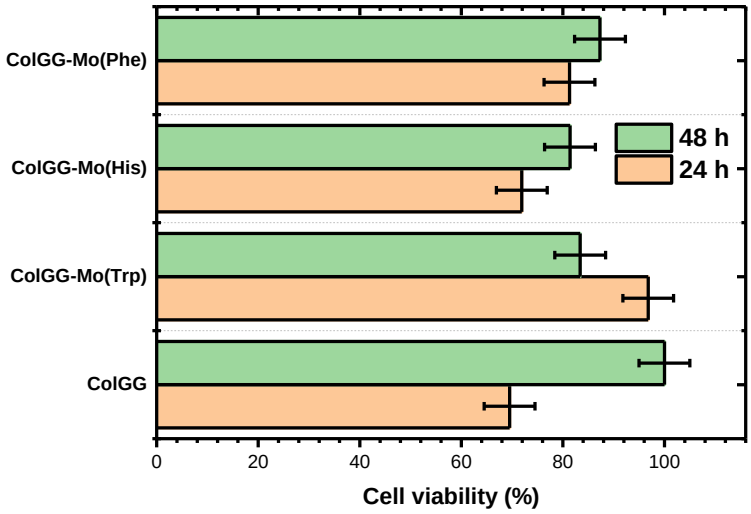

Figure 5. Viability of Porcine Dermis Fibroblasts

The images acquired by fluorescence microscopy of fibroblasts growing in contact with leaches extracted from composite hydrogels are shown in Figure 6. They reveal that ColGG and ColGG-Mo(Trp) are suitable to allow cell proliferation in the scaffold, forming dense populations of fibroblasts in contact with the degradation products of composite hydrogels, indicating again that this type of novel composite hydrogels are not cytotoxic for this type of cells important in the process of tissue remodeling and construction. These materials present noticeable enhancements compared to the control (PBS-1X), confirming the improvement of the in vitro biocompatibility caused by Mo(Trp).

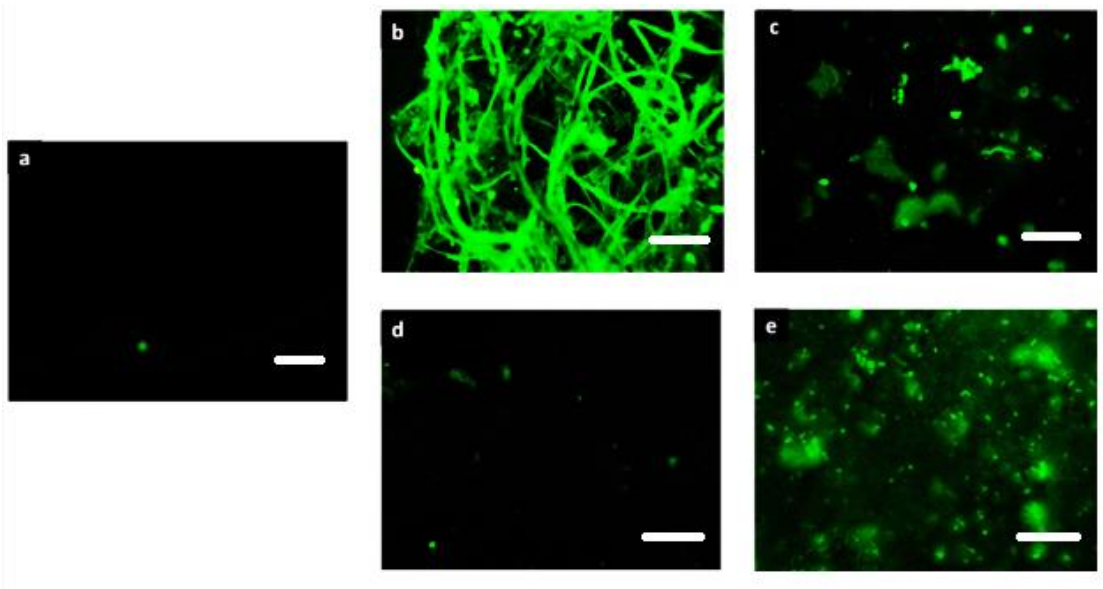

Figure 6. Proliferation of Porcine Dermis Fibroblasts Growing in contact with (a) PBS, and Leaches Extracted from (b) ColGG, (c) ColGG-Mo(Phe), (d) ColGG-Mo(His), (e) ColGG-Mo(Trp) - (The scale bar is equal to 1 µm)

3.6. Fibroblast Release Profiles

To evaluate the applicability of hydrogels containing Mo-MOFs as cell carriers, releasing profiles of fibroblast were constructed and they are shown in Figure 7. For all samples, it was observed that the optical density of the medium does not increase significantly, showing that fibroblasts tend to remain in the hydrogel matrix. This is associated with the fact that the fibroblasts are strongly adhered to the porous surfaces of these novel hydrogels, preventing their detachment under physiological release conditions. Changing the release medium to acid, alkaline or proteolytic could benefit the release of this type of cells, so that they could become target cells in localized wounds, thus optimizing the healing process. Thus, these materials are not suitable as cell carriers, but they are ideal as cell scaffolds considering the high in vitro biocompatibility observed previously.

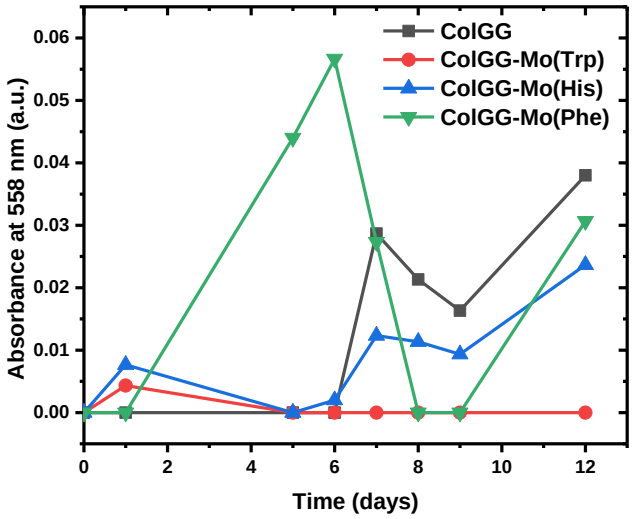

Figure 7. Fibroblast Release Profiles in PBS-1X (Physiological Condition)

4. Conclusion

The addition of Mo-MOFs to the ColGG hydrogel matrix allowed to modulate the physicochemical characteristics and the in vitro biocompatibility of the resulting composite hydrogels. Mo(Trp) was the best MOF to achieve the desired properties, observing a high water absorption capacity with a high reticulation degree, and the formation of a granular and porous microstructure suitable for cell adhesion. The MTT assay proved that the ColGG-Mo(Trp) composite increased the viability of porcine dermis fibroblasts allowing their proliferation. Considering the characteristics of ColGG-Mo(Trp) this composite hydrogel could be useful as a cell scaffold for tissue engineering and wound healing applications as wound dressings.

Declarations

Source of Funding

Consejo Nacional de Ciencia y Tecnología (CONACyT) supported this study with the grant FORDECYT-PRONACES/6660/2020.

Competing Interests Statement

The authors declare no competing financial, professional, or personal interests.

Consent for publication

The authors declare that they consented to the publication of this research work.

Authors' Contributions

All authors equally contributed to research and paper drafting.

Acknowledgement

The authors would like to acknowledge Consejo Nacional de Ciencia y Tecnología (CONACyT) for the grant FORDECYT-PRONACES/6660/2020. M. Caldera-Villalobos thanks CONACyT for the postdoctoral grant.

References

[1] N. Özen, Z. Özbaş, B. İzbudak, S. Emik, B. Özkahraman, A. Bal-Öztürk, (2022). Boric acid-impregnated silk fibroin/gelatin/hyaluronic acid-based films for improving the wound healing process. J. Appl. Polym. Sci., 139: 51715.

[2] R. Kapukaya and O. Ciloglu, (2020). Treatment of chronic wounds with polyurethane sponges impregnated with boric acid particles: A randomised controlled trial. Int. Wound J., 17: 1159–1165.

[3] P. F. Nur, T. Pınar, P. Uğur, Y. Ayşenur, E. Murat and Y. Kenan, (2021). Fabrication of polyamide 6/honey/boric acid mats by electrohydrodynamic processes for wound healing applications Polyamide 6/Honey/Boric Acid Bioactive Fibers. Mater. Today Commun., 29: 102921.

[4] L. Chen, (2019). Nursing Utility and Relevant Mechanism of Boric Acid in Promoting Wound Healing in Diabetic Mice. J. Pharm. Sci., Pages 181–185.

[5] W. Ma, T. Zhang, R. Li, Y. Niu, X. Yang, J. Liu, Y. Xu and C. M. Li, (2020). Bienzymatic synergism of vanadium oxide nanodots to efficiently eradicate drug-resistant bacteria during wound healing in vivo. J. Colloid Interface Sci., 559: 313–323.

[6] Y. Wan, J. Fang, Y. Wang, J. Sun, Y. Sun, X. Sun, M. Qi, W. Li, C. Li, Y. Zhou, L. Xu, B. Dong and L. Wang, (2021). Antibacterial Zeolite Imidazole Frameworks with Manganese Doping for Immunomodulation to Accelerate Infected Wound Healing. Adv. Healthc. Mater., 10: 2101515.

[7] Z. Wu, H. Zhuang, B. Ma, Y. Xiao, B. Koc, Y. Zhu and C. Wu, (2021). Manganese-Doped Calcium Silicate Nanowire Composite Hydrogels for Melanoma Treatment and Wound Healing. Research, Pages 1–12.

[8] S.K. Jaganathan & M. P.Mani, (2019). Electrospinning synthesis and assessment of physicochemical properties and biocompatibility of cobalt nitrate fibers for wound healing applications. An. Acad. Bras. Cienc., 91: 1–12.

[9] Q. Shi, X. Luo, Z. Huang, A. C. Midgley, B. Wang, R. Liu, D. Zhi, T. Wei, X. Zhou, M. Qiao, J. Zhang, D. Kong and K. Wang, (2019). Cobalt-mediated multi-functional dressings promote bacteria-infected wound healing. Acta Biomater., 86: 465–479.

[10] J. Li, F. Lv, J. Li, Y. Li, J. Gao, J. Luo, F. Xue, Q. Ke and H. Xu, (2020). Cobalt-based metal–organic framework as a dual cooperative controllable release system for accelerating diabetic wound healing. Nano Res., 13: 2268–2279.

[11] E.J. Baran, (1985). Química Bioinorgánica. McGraw-Hill, Madrid.

[12] J. Indrakumar, P. Balan, P. Murali, A. Solaimuthu, A. N. Vijayan and P. S. Korrapati, (2022). Applications of molybdenum oxide nanoparticles impregnated collagen scaffolds in wound therapeutics. J Trace Elem. Med. Biol., 72: 126983.

[13] X. T. He, X. Li, M. Zhang, B. M. Tian, L. J. Sun, C. S. Bi, D. K. Deng, H. Zhou, H. L. Qu, C. Wu and F. M. Chen, (2022). Role of molybdenum in material immunomodulation and periodontal wound healing: Targeting immunometabolism and mitochondrial function for macrophage modulation. Biomaterials, 283: 121439.

[14] C. E. Castañeda-Calzoncit, D. A. Cabrera-Munguia, J. A. Claudio-Rizo, D. A. Solís-Casados and C. M. López-Badillo, (2022). Biocompatible Molybdenum Complexes Based on Terephthalic Acid and Derived from PET: Synthesis and Characterization. Asian J. Appl. Sci. Technol., 06: 25–34.

[15] J. A. Claudio-Rizo, N. G. Hernandez-Hernandez, L. F. Cano-Salazar, T. E. Flores-Guía, F. N. de la Cruz-Durán, D. A. Cabrera-Munguía and J. J. Becerra-Rodríguez, (2021). Novel semi-interpenetrated networks based on collagen-polyurethane-polysaccharides in hydrogel state for biomedical applications. J. Appl. Polym. Sci., 138: 49739.

[16] E. E. Lopéz-Martínez, J. A. Claudio-Rizo, M. Caldera-Villalobos, J. J. Becerra-Rodríguez, D. A. Cabrera-Munguía, L. F. Cano-Salazar and R. Betancourt-Galindo, (2022). Hydrogels for Biomedicine Based on Semi-Interpenetrating Polymeric Networks of Collagen/Guar Gum: Applications in Biomedical Field and Biocompatibility. Macromol. Res., 30: 384–390.

[17] M. Caldera-Villalobos, D. A. Cabrera-Munguía, J. J. Becerra-Rodríguez and J. A. Claudio-Rizo, (2022). Tailoring biocompatibility of composite scaffolds of collagen/guar gum with metal-organic frameworks. RSC Adv., 12: 3672–3686.

[18] J. A. Claudio-Rizo, M. Rangel-Argote, L. E. Castellano, J. Delgado, J. L. Mata-Mata and B. Mendoza-Novelo, (2017). Influence of residual composition on the structure and properties of extracellular matrix derived hydrogels. Mater. Sci. Eng. C, 79: 793–801.

[19] B. Mendoza-Novelo, J. L. Mata-Mata, A. Vega-González, J. V. Cauich-Rodríguez and Á. Marcos-Fernández, (2014). Synthesis and characterization of protected oligourethanes as crosslinkers of collagen-based scaffolds. J. Mater. Chem. B, 2: 2874–2882.

[20] Z. H. Zhou, H. L. Wan and K. R. Tsai, (1997). Molybdenum (VI) complex with citric acid: Synthesis and structural characterization of 1 : 1 ratio citrato molybdate K2Na4[(MoO2)2O(cit) 2]·5H2O. Polyhedron, 16: 75–79.

[21] N. Barouti, C. Mainetti, L. Fontao and O. Sorg, (2015). L-tryptophan as a novel potential pharmacological treatment for wound healing via aryl hydrocarbon receptor activation. Dermatology, 230: 332–339.

[22] A. Sadiq, M. Q. Hayat, G. A. Trali and A. Javed, (2018). Effects of essential amino acid “Tryptophan” in post burn skin wound healing Atta-ur-Rahman School of Applied Biosciences (ASAB). Int. J. Biosci., 12: 147–153.

[23] L. G. Bandeira, B. S. Bortolot, M. J. Cecatto, A. Monte-Alto-Costa and B. Romana-Souza, (2015). Exogenous tryptophan promotes cutaneous wound healing of chronically stressed mice through inhibition of TNF-α and IDO activation. PLoS One, 10: 1–19.